

Coexistence of Superconductivity and Magnetism in $\text{LaFeAs}(\text{O}_{0.94}\text{F}_{0.06})$ Probed by Muon Spin Relaxation

Soshi Takeshita,¹ Ryosuke Kadono,^{1,2} Masatoshi Hiraishi,² Masanori

Miyazaki,² Akihiro Koda,^{1,2} Yohichi Kamihara,³ and Hideo Hosono^{3,4,5}

¹ *Institute of Materials Structure Science, High Energy Accelerator Research Organization, Tsukuba, Ibaraki 305-0801, Japan*

² *The Graduate University for Advanced Studies, Tsukuba, Ibaraki 305-0801, Japan*

³ *ERATO-SORST, JST, in Frontier Research Center,*

Tokyo Institute of Technology, Yokohama, Kanagawa 226-8503, Japan

⁴ *Frontier Research Center, Tokyo Institute of Technology, Yokohama, Kanagawa 226-8503, Japan*

⁵ *Materials and Structures Laboratory, Tokyo Institute of Technology, Yokohama, Kanagawa 226-8503, Japan*

(Dated: February 8, 2022)

Recent discovery of oxypnictide superconductor $\text{LaFeAs}(\text{O}_{1-x}\text{F}_x)$ (LFAO-F) with the critical temperature (T_c) of 26 K (ref.[1]) and succeeding revelation of much increased T_c upon substitution of La for other rare earth elements (such as Sm, leading to ~ 43 K ref.[2]) and application of pressure for LFAO-F (~ 43 K, ref.[3]) has triggered broad interest in the mechanism yielding relatively high T_c in this new class of compounds. While they share a feature with high- T_c cuprates that superconductivity occurs upon carrier doping to pristine compound which exhibits magnetism, they also resemble the heavy-fermion compounds in the sense that superconductivity appears in the vicinity of magnetic phase. Investigation of electronic states near the boundary between these two phases might provide some useful information on the mechanism of superconductivity, as it has been proved to be the case in many exotic superconductors. Here we show by muon experiment in the LFAO-F compound that a macroscopic phase separation into superconducting and spin glass-like magnetic phases occurs at $x = 0.06$ that is near the phase boundary, where both the magnetism and superconductivity develop simultaneously below a common $T_c \simeq 18$ K. This accordance strongly suggests intimate relationship between magnetism and superconductivity typically found in heavy-fermion systems near the quantum critical point.

One of the prevailing views for the mechanism of high- T_c in cuprate superconductors is that antiferromagnetic spin fluctuation is the predominant glue for the Cooper pairs. A similar mechanism is believed to be effective in

other class of superconductors including heavy-fermion (HF) compounds, where superconductivity appears adjacent to magnetism in various phase diagrams along with pressure, magnetic field, and carrier doping [4]. In the HF systems, this phenomenon is understood as a manifestation of so-called quantum criticality, where spin fluctuation mediating the Ruderman-Kittel-Kasuya-Yoshida (RKKY) interaction (leading to magnetic ground state) competes with the Kondo fluctuation (leading to paramagnetic state with enhanced effective mass). In such a situation, the ground states in the respective phases are connected continuously, and weak anomalies (e.g., deviation from fermi-liquid behavior) are observed near the quantum critical point. The superconductivity in the paramagnetic phase is generally understood within the framework of the BCS theory where the pairing is mediated by the strong spin fluctuation. In the case of *underdoped* cuprates, however, the situation seems more complicated because of the strong on-site Coulomb interaction among doped carriers that leads to the Mott insulating phase at zero doping. In this regard, it might be worth noting that pristine LaFeAsO seems to be metallic.

Like cuprates, LFAO-F has a layered structure, where doped carriers (electrons introduced by the substitution of O^{2-} with F^- in the La_2O_2 layers) move over the layers consisting of strongly bonded Fe and As atoms, thus the dopant and the conducting layers are separated. While it exhibits a qualitative similarity with cuprates in terms of doping phase diagram, there are certain differences, e.g. (i) T_c (> 0 for $0.4 < x < 0.12$) does not vary much with x as in cuprates known as “bell shape”, and (ii) the magnetic (spin density wave) phase shares boundary with superconducting phase near $x \simeq 0.04$. The insensitivity of T_c to x is reasonably understood by the conventional BCS theory where the condensation energy is predicted to be independent of the carrier concentration. The close proximity of magnetism and superconductivity suggests that the detailed investigation on how these two phases coexist (and compete) near the phase boundary might provide important clue for elucidating the pairing mechanism. Among various techniques, muon spin rotation/relaxation (μ SR) has the great advantage that it can be applied in systems consisting of spatially inhomogeneous multiple phases, providing information on respective phases according to their fractions. Our μ SR measurements in the LFAO-F sample with $x = 0.06$ ($T_c \simeq 18$ K) reveals that these two phases indeed coexist in a form of macroscopic phase separation, and more interestingly, that a spin glass-like magnetic phase develops in conjunction with superconductivity in the paramagnetic phase. This is in close resemblance with the situation observed in the classical HF superconductor, $CeCu_2(Si,Ge)_2$ (ref. [4, 5]), suggesting a common background for the pairing mechanism between these two systems.

While those with rare earth substitution exhibits higher T_c than that of LFAO-F, strong random fields from the rare earth ions preclude detailed study of the ground state by sensitive magnetic probes like μ SR. Therefore, we

chose the original LFAO-F system for our μ SR study. The target concentration of $\text{LaFeAs}(\text{O}_{1-x}\text{F}_x)$ is set near the phase boundary, $x = 0.06$, for which a polycrystalline sample was synthesized by a solid state reaction method. Detailed procedure for sample preparation is described in the earlier report [1]. The sample was confirmed to be mostly of single phase using X-ray diffraction method. As shown in Fig.2 (a), T_c is estimated to be ~ 18 K from the onset of diamagnetism in the magnetic susceptibility measurement. Conventional μ SR measurements were performed using the LAMPF spectrometer installed on the M15 beamline of TRIUMF, Canada. For longitudinal field (LF) measurement, a magnetic field was applied parallel to the muon beam direction (\hat{z} -axis) that was also parallel to the initial muon spin direction [$\vec{P}_\mu(0) \parallel \hat{z}$]. During the measurement under zero field (ZF), residual magnetic field at the sample position was reduced below 10^{-6} T with $\vec{P}_\mu(0) \parallel \hat{z}$. Time-dependent muon polarization [$P_z(t) = \hat{z} \cdot \vec{P}_\mu(t)$] was monitored by measuring decay-positron asymmetry along the \hat{z} -axis, $A(t) [\propto P_z(t)]$. Transverse field (TF) condition was realized by rotating the initial muon polarization so that $\vec{P}_\mu(0) \perp \hat{z}$, where the asymmetry was monitored along the \hat{x}/\hat{y} -axes. All the measurements under magnetic field were made by cooling down the sample to the target temperature after the field was settled.

ZF- μ SR is the most sensitive technique to examine magnetism in any form, where the development of local magnetic moments leads to either spontaneous oscillation (for long-range order) or exponential damping (inhomogeneous local magnetism) of $A(t)$. Figure 1 (a) shows the ZF- μ SR time spectra collected at various temperatures below 30 K. The spectrum at 30 K ($> T_c$) exhibits a Gaussian-like relaxation due to weak random local fields from nuclear magnetic moments, indicating that the entire sample is in the paramagnetic state. Meanwhile, the spectrum at 2 K is split into two components, one that exhibits a steep relaxation and the other that remains to show a Gaussian-like relaxation. This indicates that there is a finite fraction of implanted muons that sense the hyperfine fields from local electronic moments. The absence of oscillatory signal implies that the hyperfine field is highly inhomogeneous, so that the local magnetism is characterized by strong randomness or spin fluctuation. The fractional yield of the component showing steep relaxation is as large as 0.25 (see below), which is hardly attributed to impurity and therefore implies that the sample exhibits a macroscopic phase separation into two phases.

The magnitude of the hyperfine field is evaluated by observing the response of μ SR spectra upon the variation of longitudinal field. (Although the sample falls into the mixed state below T_c , the flux lines are parallel to $\vec{P}_\mu(t)$, where the small inhomogeneity of the field due to magnetic vortices is negligible.) As observed in Fig. 1 (b), the relaxation in the paramagnetic component is quenched by applying a weak magnetic field ($\simeq 5$ mT), which is perfectly explained by the suppression of nuclear dipolar fields ($< \sim 1$ mT). Meanwhile, the faster relaxation (seen

for $0 < t < 1 \mu\text{s}$) due to the magnetic phase is recovered only gradually over a field range of $10^{1\sim 2}$ mT, and one may notice that there still remains a slow relaxation even at the highest field of 60 mT. This residual depolarization under LF is a clear sign that the local spins are slowly fluctuating, leading to spin-lattice relaxation of $\vec{P}_\mu(t)$. The detailed analysis is made considering these two components coming from the magnetic phase (see below).

Under a transverse field, implanted muons experience inhomogeneity of the field $[B_z(\mathbf{r})]$ due to flux line lattice formation below T_c that leads to relaxation additional to those observed under zero field. Figure 1 (c) shows TF- μSR time spectra (envelop part of the oscillation) at various temperatures obtained under a field of 50 mT, where one can clearly observe that the relaxation becomes faster than that in Fig. 1 (a) below T_c . The steeply relaxing component observed in Fig. 1 (a) is also visible (although the coarse binning of the spectra for extracting the envelop part makes it slightly obscure), indicating that the corresponding part of the sample remains magnetic.

Considering the presence of magnetic phase besides paramagnetic (=superconducting below T_c) phase, we take a special precaution to analyze both TF and ZF/LF μSR spectra in a consistent manner. For the determination of physical parameters describing the behavior of signals from the magnetic phase, we first analyze LF spectra at 2 K using the χ -square minimization fit with the following relaxation function,

$$A(t) = [A_1 + \sum_{i=2}^3 A_i \exp(-\Lambda_i t)] \cdot G_{\text{KT}}(\delta_N : t), \quad (1)$$

where $G_{\text{KT}}(\delta_N : t)$ is the Kubo-Toyabe relaxation function to describe the Gaussian damping due to random local fields from nuclear moments (with δ_N being the linewidth) [6], A_1 is the initial asymmetry for paramagnetic phase, $A_{2,3}$ are those for the magnetic phase with $\Lambda_{2,3}$ being the corresponding relaxation rate described by the Redfield relation,

$$\Lambda_i = \frac{2\delta_i^2 \nu_i}{\nu_i^2 + \omega_\mu^2} \quad (i = 2, 3), \quad (2)$$

where $\omega_\mu = \gamma_\mu H_{\text{LF}}$, γ_μ is the muon gyromagnetic ratio ($= 2\pi \times 135.53$ MHz/T), H_{LF} is the longitudinal field, $\delta_{2,3}$ are mean values of the hyperfine fields exerting on muons from local electronic moments, $\nu_{2,3}$ are the fluctuation rate of the hyperfine field. The solid curves in Fig. 1 (b) show the result of analysis where all the spectra at different fields are fitted simultaneously using eqs. (1), (2) with common parameter values (except ω_μ that is fixed to respective value for each spectrum), which show excellent agreement with all the spectra. The deduced parameters are listed in Table I. The volume fraction of the paramagnetic and magnetic phases estimated from the ratio of A_i are approximately 75% ($= A_1 / \sum A_i$) and 25% [$= (A_2 + A_3) / \sum A_i$], respectively. Since no impurity phase with fraction as large as 25% is detected by X-ray diffraction measurement, it is concluded that this magnetic phase is intrinsic.

In the analysis of temperature dependent TF spectra, we used the following relaxation function,

$$A(t) = \exp\left(-\frac{1}{2}\delta_N^2 t^2\right)[A_1 \exp(-\delta_s^2 t^2) \cos(2\pi f_s t + \phi) + (A_2 + A_3) \exp(-\Lambda_m t) \cos(2\pi f_m t + \phi)], \quad (3)$$

where A_i and δ_N are fixed to the values obtained by analyzing ZF/LF- μ SR spectra. The first component in the above equation represents the contribution of flux line lattice formation in superconducting phase, where δ_s corresponds to the linewidth $\sigma_s = \sqrt{2}\delta_s = \gamma_\mu \langle (B(\mathbf{r}) - B_0)^2 \rangle^{1/2}$ [with B_0 being the mean value of $B(\mathbf{r})$], while the second term represents the relaxation in the magnetic phase. Here, the relaxation rate for the latter is represented by a single value Λ_m (instead of $\Lambda_{2,3}$), as it turns out that these two components observed under LF are hardly discernible in TF- μ SR spectra. (This does not affect the result of the analysis, because the amplitude is fixed to $A_1 + A_3$ so that Λ_m may represent a mean value.) The fit analysis using the above form indicates that all the spectra are perfectly reproduced while the partial asymmetry is fixed to the value determined by ZF- μ SR spectra. This endorses the presumption that the paramagnetic phase becomes superconducting below T_c . The result of analysis is summarized in Fig. 2, together with the result of dc magnetization measured on the sample from the same batch as that used for μ SR.

It is interesting to note in Fig. 2 (b) that, while the central frequency in the superconducting phase (f_s) does not show much change below $T_c \simeq 18$ K probably due to a large magnetic penetration depth (it is indeed large, see below), that in the magnetic phase (f_m) exhibits a clear shift to the negative direction below T_c . The magnitude of the shift is as large as $\sim 1\%$ and thus readily identified despite a relatively low external field of 50 mT. As shown in Fig. 2 (c), the relaxation rate in the magnetic phase (Λ_m) also develops below T_c in accordance with the frequency shift, demonstrating that a spin glass-like magnetism sets in below T_c . Here, we note that the development of magnetic phase is already evident in the ZF/LF- μ SR spectra, and results are fully consistent with each other. The onset of superconductivity below T_c is also confirmed by the increase of δ_s as observed in Fig. 2 (c). This remarkable accordance of onset temperature between magnetism and superconductivity strongly suggests that there is an intrinsic relationship between superconducting and magnetic phase that leads to a common characteristic temperature.

In Fig. 2 (b), the temperature dependence of σ_s is compared with theoretical predictions for a variety of models with different order parameters. The weak coupling BCS model (s -wave, single gap) apparently fails to reproduce the present data, as they exhibit a tendency to vary with temperature over the region $T/T_c < 0.4$. Although fit by a two-gap model [7] shown by dotted line seems to exhibit reasonable agreement with data, the deduced gap

parameters ($2\Delta_i/k_B T_c$) are largely inconsistent with the prediction of the weak coupling BCS model (see Table II). These observations strongly suggests that the superconducting order parameter is not described by s-wave symmetry with single gap. When a power law, $\sigma_s = \sigma_0[1 - (T/T_c)^\beta]$, is used to reproduce the data by fit analysis, we obtain a curve shown by the broken line in Fig. 2 (b) with the exponent $\beta \simeq 2$. This is in good accord with the case of *d*-wave symmetry at the dirty limit.

In the limit of extreme type II superconductors [i.e., $\lambda/\xi \gg 1$, where λ is the effective London penetration depth and $\xi = \sqrt{\Phi_0/(2\pi H_{c2})}$ is the Ginzburg-Landau coherence length, Φ_0 is the flux quantum, and H_{c2} is the upper critical field], σ_s is determined by λ using a relation [8], $\sigma_s = 2.74 \times 10^{-2}(1-h) [1 + 3.9(1-h)^2]^{1/2} \Phi_0 \lambda^{-2}$, where $h = H_{TF}/H_{c2}$, and H_{TF} is the magnitude of external field. From the value of σ_s extrapolated to $T = 0$ and taking $H_{c2} \simeq 50$ T (ref. [9]), we obtain $\lambda = 595(3)$ nm. Because of large anisotropy expected from the layered structure of this compound, λ in the polycrystalline sample would be predominantly determined by in-plane penetration depth (λ_{ab}). Using a formula, $\lambda = 1.31\lambda_{ab}$ for such situation [10], we obtain $\lambda_{ab} = 454(2)$ nm. This value coincides with that expected from the empirical relation between λ_{ab}^{-2} vs T_c observed in hole-doped cuprate superconductors [11, 12]. However, this may not be uniquely attributed to the superfluid density (n_s) because λ depends not only n_s but also on the effective mass, $\sigma(0) \propto \lambda^{-2} = n_s e^2 / m^* c^2$.

Until now, μ SR study of LFAO-F has been made by a number of groups. According to those preliminary reports, no clear sign of magnetism is observed in the sample with $x = 0.08$ [12], 0.075, and 0.10 [13] (except a weak relaxation observed for $x = 0.10$ in ZF- μ SR spectra below T_c and an unidentified additional relaxation observed in TF- μ SR spectra for $x = 0.075$).

The phase separation observed in LaFeAs(O_{0.94}F_{0.06}) exhibits a close resemblance to so-called magnetic “A-phase” in CeCu₂Si₂ (ref. [14]), where a spatial phase separation into superconducting and A-phase is observed near the boundary of superconducting and antiferromagnetic phases. The A-phase shares a feature of spin glass-like magnetism with the magnetic phase observed in the present LFAO-F sample. It is known for CeCu₂Si₂ that the partitioning of those two phases changes drastically upon small off-stoichiometry of Ce or Cu from the nominal formula. Further study on the dependence of fractional yield for the magnetic phase with varying x (in small steps near the phase boundary) would provide more insight into the true nature of coexistence/competition of these phases and the mechanism of superconductivity itself that is working behind the coexistence/competition.

-
- [1] Kamihara, Y., Watanabe, T., Hirano, M. & Hosono, H. Iron-Based Layered Superconductor $\text{La}[\text{O}_{1-x}\text{F}_x]\text{FeAs}$ ($x=0.05-0.12$) with $T_c=26$ K. *J. Am. Chem. Soc.* **130**, 3296-3297 (2008).
- [2] Chen, X. H., Wu, T., Liu, R. H., Chen, H., & Fang, D. F. Superconductivity at 43 K in $\text{SmFeAsO}_{1-x}\text{F}_x$. *Nature* **453**, 761-762 (2008).
- [3] Takahashi, H., et al. Superconductivity at 43 K in an iron-based layered compound $\text{LaO}_{1-x}\text{F}_x\text{FeAs}$. *Nature* **453**, 376-378 (2008).
- [4] Monthoux, P., Pines, D., & Lonzarich, G. G. Superconductivity without phonons. *Nature* **450**, 1177-1183 (2007).
- [5] Jaccard, D., Behnia, K. & Sierro, J. Pressure induced heavy fermion superconductivity of CeCu_2Ge_2 . *Phys. Lett. A* **163**, 475-480 (1992).
- [6] Hayano, R. S., et al. Zero- and low-field spin relaxation studied by positive muons. *Phys. Rev. B* **20**, 850-859 (1979).
- [7] Bouquet, F., et al. Phenomenological two-gap model for the specific heat of MgB_2 . *Europhys. Lett.* **56**, 856-862 (2001).
- [8] Brandt, E. H., Flux distribution and penetration depth measured by muon spin rotation in high- T_c superconductors. *Phys. Rev. B* **37**, 2349-2352 (1988).
- [9] Hunte, F., et al. Two-band superconductivity in $\text{LaFeAsO}_{0.89}\text{F}_{0.11}$ at very high magnetic fields. *Nature* **453**, 903-905 (2008).
- [10] Fesenko, V. I., Gorbunov, V. N. & Smilga, V. P. Analytical properties of muon polarization spectra in type-II superconductors and experimental data interpretation for mono- and polycrystalline HTSCs. *Physica C* **176**, 551-558 (1991).
- [11] Uemura, Y. J., et al. Systematic variation of magnetic-field penetration depth in high- T_c superconductors studied by muon-spin relaxation. *Phys. Rev. B* **38**, 909-912 (1988).
- [12] Carlo, J. P., et al. μSR studies of $\text{RE}(\text{O},\text{F})\text{FeAs}$ ($\text{RE}=\text{La}, \text{Nd}, \text{Ce}$) and LaOFeP systems: possible incommensurate/stripe magnetism and superfluid density. (<http://arxiv.org/abs/0805.2186>) (2008).
- [13] Luetkens, H., et al. Field and Temperature Dependence of the Superfluid Density in $\text{LaO}_{1-x}\text{F}_x\text{FeAs}$ Superconductors: A Muon Spin Relaxation Study. (<http://arxiv.org/abs/0804.3115>) (2008).
- [14] Feyerherm, R., et al. Competition between magnetism and superconductivity in CeCu_2Si_2 . *Phys. Rev. B* **56**, 699-710 (1997).

Acknowledgements

We would like to thank the TRIUMF staff for their technical support during the μSR experiment. This work was partially supported by the KEK-MSL Inter-University Program for Oversea Muon Facilities and a Grant-in-Aid for Creative Scientific Research on Priority Areas by the Ministry of Education, Culture, Sports, Science and Technology, Japan.

Competing financial interests

The authors declare that they have no competing financial interests.

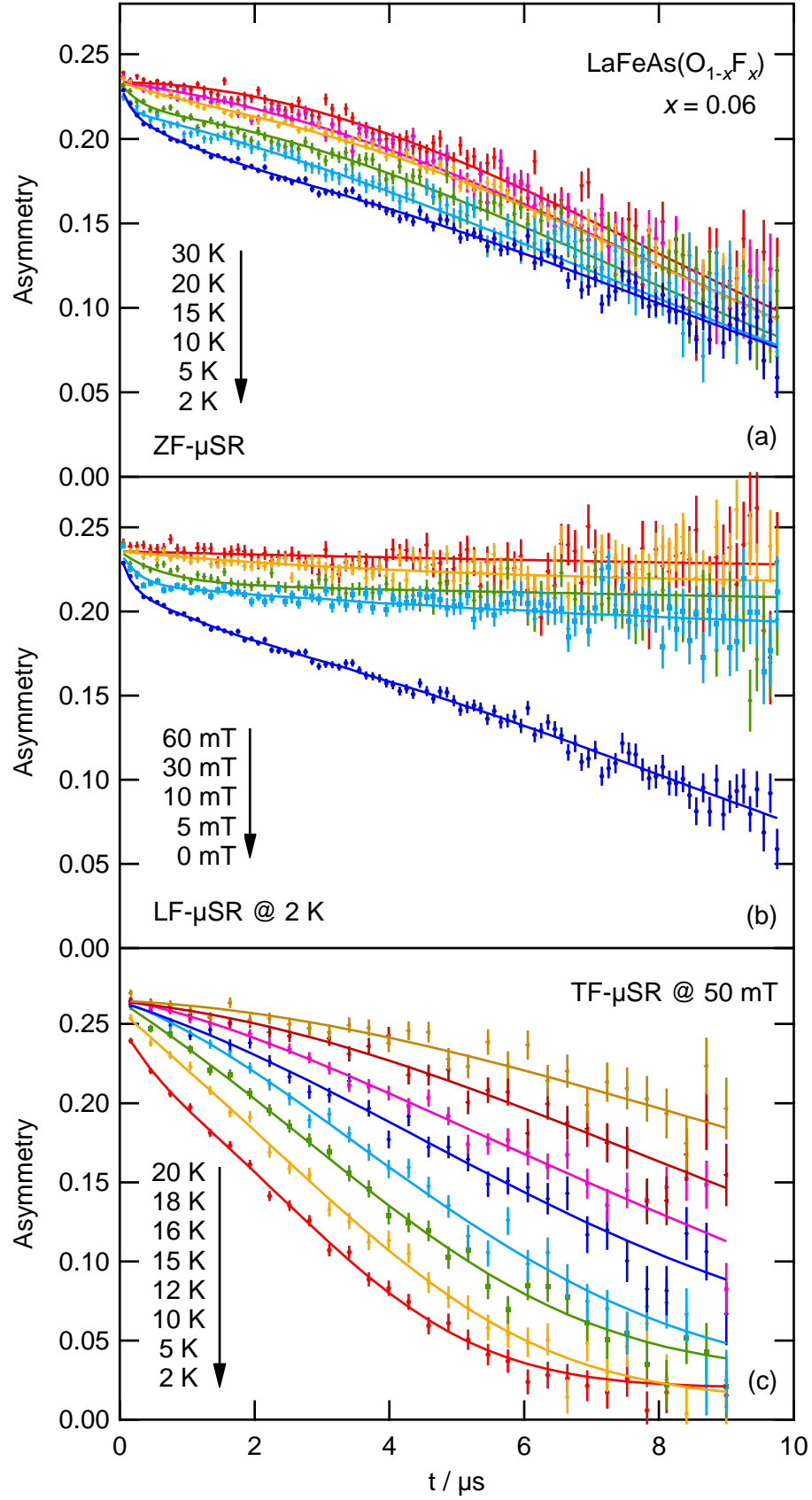


FIG. 1: μ SR time spectra observed in LaFeAs(O_{1-x}F_x) with $x = 0.06$ under (a) ZF, (b) LF, and (c) TF. The order of spectra is shown by the arrow. The spectra in (c) are plotted on a rotating reference frame of 6.78 MHz to extract the envelop function.

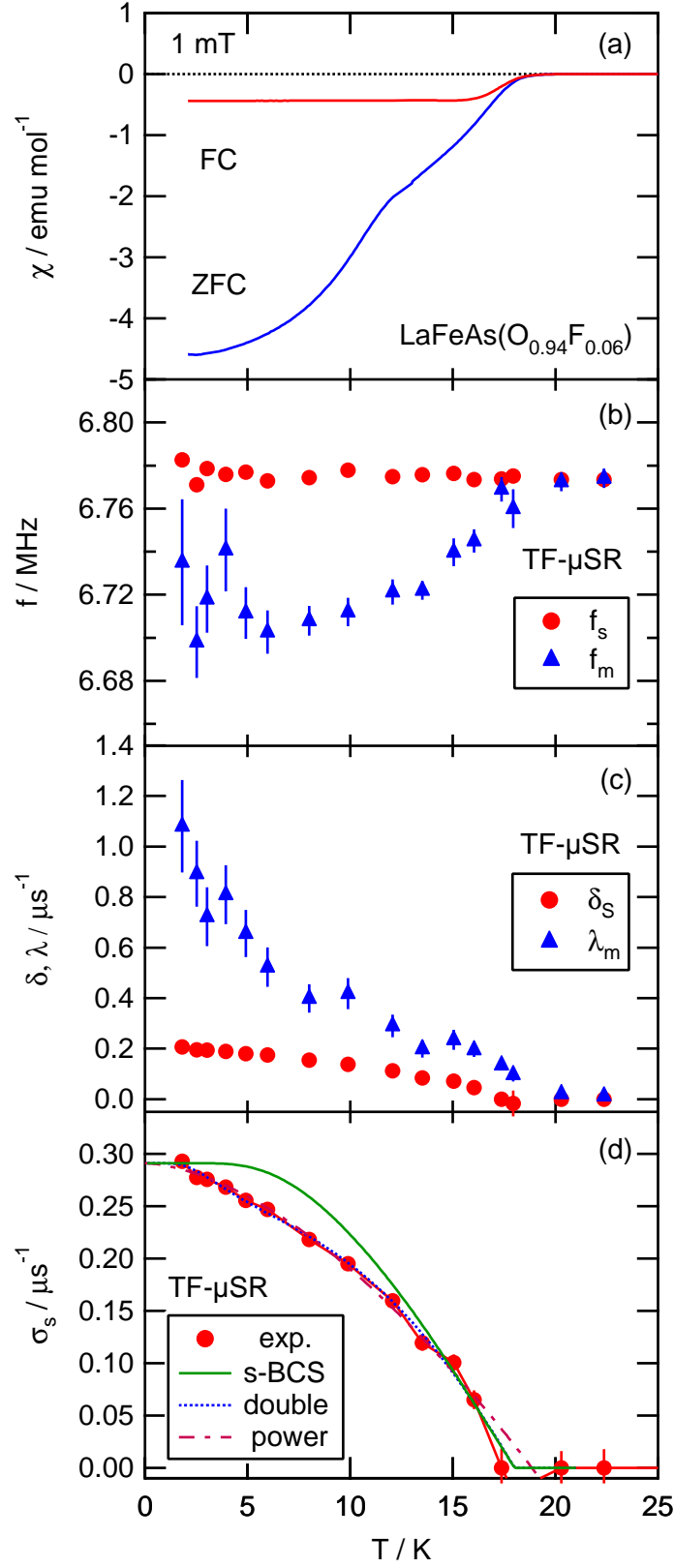


FIG. 2: (a) Temperature dependence of dc magnetic susceptibility measured at 1mT. (b)-(c) Physical parameters deduced by analyzing TF- μ SR spectra, where the central frequency (b) and relaxation rate (c) are shown as a function of temperature for superconducting (f_s , δ_s) and magnetic (f_m , λ_m) phases. (d) The temperature dependence of the linewidth that is proportional to the superfluid density. Lines are fits by various models (see text).

i	A_i	fraction	δ_i (μs^{-1})	ν_i (μs^{-1})
1	0.178(2),	75.4%	–	–
2	0.039(2),	16.5%	0.71(5)	1.7(2)
3	0.019(1),	8.1%	3.9(3)	4(1)

TABLE I: Physical parameters obtained from LF- μ SR spectra at 2 K by analysis using eq. (1).

Two-gap		Power law	
T_c (K)	18.0(5)	T_c (K)	18.9(4)
$\sigma(0)$ (μs^{-1})	0.291(5)	$\sigma(0)$ (μs^{-1})	0.291(4)
w	0.73(6)	β	1.7(1)
$2\Delta_1/k_B T_c$	2.6(3)		
$2\Delta_2/k_B T_c$	1.1(3)		

TABLE II: Parameters to define the lines in Fig. 2(d).